

Theory of optical phase conjugation in Kerr media

Henk F. Arnoldus

Department of Physics and Astronomy, Mississippi State University, P.O. Drawer 5167, Mississippi State, Mississippi 39762-5167

Thomas F. George

Departments of Chemistry and Physics, Washington State University, Pullman, Washington 99164-1046

(Received 16 September 1994)

Optical phase conjugation by four-wave mixing in a Kerr medium is considered. Two strong counter-propagating lasers pump a nonlinear medium in which they excite the third-order polarization. Mixing with a weak incident field then generates the phase-conjugated image of that field. It is shown how the polarization of the pumps and the tensorial nature of the nonlinear interaction can be accounted for by a geometrical polarization tensor. The electric field is shown to obey two coupled wave equations, which couple a positive- and negative-frequency component of the field. These wave equations allow plane-wave solutions, and we derive the dispersion relation for the wave vectors of these modes. By matching the field of such a mode across the boundaries of the medium to an external incident field, we are able to obtain analytically the Fresnel coefficients for reflection and transmission. Our expressions reduce to earlier results in the appropriate limits.

PACS number(s): 42.65.Hw, 41.20.Bt

I. INTRODUCTION

Phase conjugation of an optical wave front was first demonstrated experimentally by Zel'dovich and co-workers [1]. The wave front of a laser beam was distorted by letting it pass through an etched glass plate, and subsequently this wave was sent into a Brillouin cell with methane gas. When the backscattered light was passed through the same glass plate, the distortions disappeared. From this it was concluded that the Brillouin mirror operated as a phase conjugator (PC). This conclusion is based on the fact that complex conjugation of the phase of a wave front is formally identical to time reversal [2-6]. After this experimental milestone, the field of optical phase conjugation has developed rapidly. Phase conjugation in liquid CS_2 by Brillouin scattering [7] and Raman scattering [8] was observed, and later it was proposed to construct a PC based on four-wave mixing (FWM) in nonlinear liquids or crystals [9,10]. The advantages of four-wave mixing, as compared to Brillouin scattering, are that the response time of the medium is negligible, the frequency shift with the acoustic frequency of the medium is absent, and the required laser power is much less. Four-wave mixing PC's were demonstrated shortly afterwards [11-13]. The most favorable nonlinear media for phase conjugation are photorefractive crystals like BaTiO_3 or LiNbO_3 , and their operation has been studied extensively [14-25]. Although four-wave mixing and the generation of phase-conjugated radiation in this process are well understood in principle, the theoretical developments rely on many simplifying assumptions. Most notable approximations are the slowly varying amplitude approximation for the waves in the medium, the neglect of the vector character of the electromagnetic field and the tensorial nature of the nonlinear interaction, and the dependence on the polarization and the angle of incidence (by assuming near-normal

incidence). Also the influence of a nonunity dielectric constant ϵ is usually not taken into account (by assuming perfect transparency for the crystal). In this paper we do not make any of these simplifications, and present an exact and analytical solution of Maxwell's equations for a four-wave mixing PC. We shall also allow the incident field to have evanescent components, as is, for instance, the case of radiation emitted by a dipole near the surface of the medium [26,27]. The dielectric constant will be assumed to be real, so that there is no loss in the medium.

The setup under consideration and the choice of coordinate system are illustrated in Fig. 1. Two strong monochromatic laser beams (the pumps) illuminate the sides of a nonlinear medium with thickness Δ and length L in the propagation direction of the pumps. A weak field is incident on the layer from the positive- z direction, and the FWM process inside the medium generates the phase-conjugated image of this field. Since the coupling of the various waves through the nonlinear interaction is tensorial, the operation of the PC will depend on the polarization of the pumps. We shall assume the pumps to be

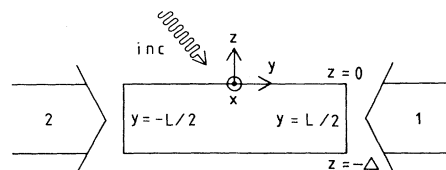


FIG. 1. Schematic setup of a PC operating by FWM. The crystal is bounded by the $z=0$ and $z=-\Delta$ planes and irradiated by two strong laser beams, propagating parallel to the xy plane, and they illuminate the medium at $y=L/2$ and $y=-L/2$. Also shown is the weak incident field which will be phase conjugated by the PC.

linearly polarized in the z direction, and for the electric components of the two fields we take, respectively,

$$\begin{aligned}\vec{E}(\vec{r}, t)_1 &= \vec{e}_z \text{Re} \bar{E} e^{-i(\bar{k}_y + \bar{\omega}t)}, \\ \vec{E}(\vec{r}, t)_2 &= \vec{e}_z \text{Re} \bar{E} e^{i(\bar{k}_y - \bar{\omega}t)},\end{aligned}\quad (1.1)$$

with $\bar{\omega} = c\bar{k}$ and \bar{E} the (complex) amplitude. Since the amplitudes are taken to be equal, both pumps have the same intensity, but this also implies a phase-matching condition. It can be shown that a phase shift between the pumps reduces the efficiency in case of a nonunity dielectric constant.

II. MAXWELL'S EQUATIONS

Radiation inside and outside the PC is represented by its electric and magnetic field components $\vec{E}(\vec{r}, t)$ and $\vec{B}(\vec{r}, t)$, respectively, and charges and currents in the medium are accounted for by a polarization field $\vec{P}(\vec{r}, t)$. It is convenient to work with the Fourier-transformed electric field, defined as

$$\hat{E}(\vec{r}, \omega) = \int_{-\infty}^{\infty} dt e^{i\omega t} \vec{E}(\vec{r}, t), \quad \omega \text{ real}. \quad (2.1)$$

Since $\vec{E}(\vec{r}, t)$ is real, it follows that its Fourier components at positive and negative frequencies are related as

$$\hat{E}(\vec{r}, \omega)^* = \hat{E}(\vec{r}, -\omega). \quad (2.2)$$

Other time-dependent quantities transform similarly. Maxwell's equations in the Fourier domain, relating the three fields, can be written as

$$\vec{\nabla} \times [\vec{\nabla} \times \hat{E}(\vec{r}, \omega)] - \frac{\omega^2}{c^2} \hat{E}(\vec{r}, \omega) = \frac{\omega^2}{\epsilon_0 c^2} \hat{P}(\vec{r}, \omega), \quad (2.3)$$

$$\hat{B}(\vec{r}, \omega) = -\frac{i}{\omega} \vec{\nabla} \times \hat{E}(\vec{r}, \omega). \quad (2.4)$$

This set of two equations is equivalent to the more common set of four equations [28]. In the next section it will be shown that the polarization is a function of $\hat{E}(\vec{r}, \omega)$ inside the medium, and outside the material we set $\hat{P}(\vec{r}, \omega)$ equal to zero. Then Eq. (2.3) becomes an equation for $\hat{E}(\vec{r}, \omega)$ only, and its solution determines the magnetic field through Eq. (2.4). At $\hat{z} = 0$, $z = -\Delta$, $y = -L/2$, and $y = L/2$ the components $(\hat{E} + \hat{P}/\epsilon_0)_\perp$, \hat{E}_\parallel , and \hat{B} must be continuous across these boundaries. Furthermore, the solution for $\hat{E}(\vec{r}, \omega)$ is restricted by condition (2.2).

III. POLARIZATION

The polarization in a nonmetallic medium is induced by the electric field, and the most general (local and causal) relation in the Fourier domain is [29,30]

$$\hat{P}(\vec{r}, \omega) = \epsilon_0 \sum_{n=1}^{\infty} \frac{1}{(2\pi)^{n-1}} \int_{-\infty}^{\infty} d\omega_1 \cdots \int_{-\infty}^{\infty} d\omega_n \delta(\omega - \omega_1 - \cdots - \omega_n) \hat{\chi}^{(n)}(\omega_1, \dots, \omega_n) : \hat{E}(\vec{r}, \omega_1) \cdots \hat{E}(\vec{r}, \omega_n). \quad (3.1)$$

Here, $\hat{\chi}^{(n)}(\omega_1, \dots, \omega_n)$ is the n -fold Fourier transform of the n th-order susceptibility function, which is a Cartesian tensor of rank $n+1$, and the colon in Eq. (3.1) indicates the tensor product with the n electric-field vectors following the colon. It is assumed that the medium is homogeneous, so that $\hat{\chi}^{(n)}$ is independent of \vec{r} .

As a first simplification we assume that the medium is inversion invariant, which implies that the even susceptibility functions $\hat{\chi}^{(2)}, \hat{\chi}^{(4)}, \dots$ are identically zero. Furthermore, the values of $\hat{\chi}^{(n)}$ decrease very rapidly with increasing n , so we only need to retain the $n=1$ and $n=3$ terms in Eq. (3.1). We write

$$\hat{P}(\vec{r}, \omega) = \hat{P}(\vec{r}, \omega)^{(1)} + \hat{P}(\vec{r}, \omega)^{(3)}, \quad (3.2)$$

in obvious notation. The two remaining tensors $\hat{\chi}^{(1)}$ and $\hat{\chi}^{(3)}$ have 9 and 81 Cartesian components, respectively, which are all different functions of one and three frequencies, respectively. As a second assumption we take the medium to be isotropic. Then it can be shown that $\hat{\chi}^{(1)}$

has only three nonzero components, which are all equal, and that $\hat{\chi}^{(3)}$ has 21 nonzero components. Among these 21 components there are only three different ones, which are not even independent. It can then be shown that the two tensor products reduce to

$$\hat{\chi}^{(1)}(\omega_1) : \vec{a} = \hat{\chi}_{xx}^{(1)}(\omega_1) \vec{a}, \quad (3.3)$$

$$\begin{aligned}\hat{\chi}^{(3)}(\omega_1, \omega_2, \omega_3) : \vec{a} \vec{b} \vec{c} &= \hat{\chi}_{xyyy}^{(3)}(\omega_1, \omega_2, \omega_3) (\vec{b} \cdot \vec{c}) \vec{a} \\ &+ \hat{\chi}_{xyxy}^{(3)}(\omega_1, \omega_2, \omega_3) (\vec{a} \cdot \vec{c}) \vec{b} \\ &+ \hat{\chi}_{xyyx}^{(3)}(\omega_1, \omega_2, \omega_3) (\vec{a} \cdot \vec{b}) \vec{c},\end{aligned}\quad (3.4)$$

for arbitrary vectors \vec{a} , \vec{b} , and \vec{c} . These two expressions are substituted into Eq. (3.1), and we use the intrinsic permutation symmetry of tensor components to change integration variables. We then obtain for the two contributions to the polarization

$$\hat{P}(\vec{r}, \omega)^{(1)} = \epsilon_0 \hat{\chi}_{xx}^{(1)}(\omega) \hat{E}(\vec{r}, \omega), \quad (3.5)$$

$$\hat{P}(\vec{r}, \omega)^{(3)} = \frac{3\epsilon_0}{4\pi^2} \int_{-\infty}^{\infty} d\omega_1 \int_{-\infty}^{\infty} d\omega_2 \int_{-\infty}^{\infty} d\omega_3 \delta(\omega - \omega_1 - \omega_2 - \omega_3) \hat{\chi}_{xyyy}^{(3)}(\omega_1, \omega_2, \omega_3) \hat{E}(\vec{r}, \omega_1) [\hat{E}(\vec{r}, \omega_2) \cdot \hat{E}(\vec{r}, \omega_3)], \quad (3.6)$$

which only involves two tensor components, and a dot product rather than a tensor product. This great simplification was derived from symmetry only.

It is convenient to introduce the dielectric constant of the medium,

$$\epsilon(\omega) = 1 + \hat{\chi}_{xx}^{(1)}(\omega), \quad (3.7)$$

which obeys the relation $\epsilon(\omega)^* = \epsilon(-\omega)$. Equation (2.3) for the electric field inside the medium then becomes

$$\vec{\nabla} \times [\vec{\nabla} \times \hat{E}(\vec{r}, \omega)] - \epsilon(\omega) \frac{\omega^2}{c^2} \hat{E}(\vec{r}, \omega) = \frac{\omega^2}{\epsilon_0 c^2} \hat{P}(\vec{r}, \omega)^{(3)}, \quad (3.8)$$

with $\hat{P}^{(3)}$ given by Eq. (3.6). This nonlinear term couples every Fourier spectral component $\hat{E}(\vec{r}, \omega)$ with every other one.

IV. WEAK INCIDENT FIELD

A major complication with expression (3.6) for $\hat{P}^{(3)}$ is that \hat{E} represents the total electric field at position \vec{r} in the medium. It contains contributions from (i) the external pump fields which propagate through the medium, (ii) multiple reflections of these fields at the boundaries $y = \pm L/2$ due to $\epsilon \neq 1$, (iii) the field incident from the region $z > 0$, and (iv) any radiation which is generated by the nonlinear interaction. The strong pumps have only nonzero Fourier components at $\omega = \pm \bar{\omega}$, and hence these are represented by δ functions. The linear interaction in the medium does not shift these frequencies, and the nonlinear interaction couples these fields to other spectral components, but such that the generated fields are weak compared to the pump fields. In contrast, the weak incident field can have any spectral composition, but both the linear and nonlinear interactions can only produce new weak fields inside the medium. Consequently, the electric field inside the layer must have the form

$$\hat{E}(\vec{r}, \omega) = \hat{E}(\vec{r}, \omega)' + \bar{e}(\vec{r})\delta(\omega - \bar{\omega}) + \bar{e}(\vec{r})^*\delta(\omega + \bar{\omega}), \quad (4.1)$$

with \hat{E}' weak and both \bar{e} terms strong, although the form of $\bar{e}(\vec{r})$ has yet to be determined.

Then we substitute expression (4.1) into Eq. (3.6) for the three different values of ω . This yields terms of the form $(E')^3$, $(E')^2e$, $E'e^2$, and e^3 . Under the assumption of a weak incident field we can then neglect the terms of the form $(E')^3$ and $(E')^2e$, since they will be small compared to the remaining terms. If we then carry out the integrations over the three frequencies, we obtain

$$\begin{aligned} \hat{P}(\vec{r}, \omega)^{(3)} &= \bar{p}(\vec{r})\delta(\omega - \bar{\omega}) + \bar{p}(\vec{r})^*\delta(\omega + \bar{\omega}) \\ &+ \bar{q}(\vec{r})\delta(\omega - 3\bar{\omega}) + \bar{q}(\vec{r})^*\delta(\omega + 3\bar{\omega}) \\ &+ (12 \text{ terms of order } E'e^2), \end{aligned} \quad (4.2)$$

with

$$\begin{aligned} \bar{p}(\vec{r}) &= \frac{3\epsilon_0}{4\pi^2} \{ \hat{\chi}_{xyyy}^{(3)}(\bar{\omega}, \bar{\omega}, -\bar{\omega}) + \hat{\chi}_{xyyy}^{(3)}(\bar{\omega}, -\bar{\omega}, \bar{\omega}) \} \\ &\times \{ \bar{e}(\vec{r}) \cdot \bar{e}(\vec{r})^* \} \bar{e}(\vec{r}) \\ &+ \frac{3\epsilon_0}{4\pi^2} \hat{\chi}_{xyyy}^{(3)}(-\bar{\omega}, \bar{\omega}, \bar{\omega}) \{ \bar{e}(\vec{r}) \cdot \bar{e}(\vec{r}) \} \bar{e}(\vec{r})^*, \end{aligned} \quad (4.3)$$

$$\bar{q}(\vec{r}) = \frac{3\epsilon_0}{4\pi^2} \hat{\chi}_{xyyy}^{(3)}(\bar{\omega}, \bar{\omega}, \bar{\omega}) \{ \bar{e}(\vec{r}) \cdot \bar{e}(\vec{r}) \} \bar{e}(\vec{r}). \quad (4.4)$$

The p terms in Eq. (4.2) have δ functions at the same frequencies as the pumps, and they represent a nonlinear contribution to the polarization at these frequencies, in addition to the linear part which is already accounted for by the dielectric constant. The q terms occur at $\omega = \pm 3\bar{\omega}$, and they are responsible for third-harmonic generation by four-wave mixing in the medium. The remaining twelve weak-field terms will generate the phase-conjugate image of the incident field, among additional side effects.

From Eq. (4.2) it follows that $\hat{P}^{(3)}$ has the form

$$\hat{P}(\vec{r}, \omega)^{(3)} = \hat{P}(\vec{r}, \omega)' + \bar{p}(\vec{r})\delta(\omega - \bar{\omega}) + \bar{p}(\vec{r})^*\delta(\omega + \bar{\omega}), \quad (4.5)$$

just as the electric field in Eq. (4.1). Then Maxwell's equation (3.8) is certainly satisfied if both

$$\vec{\nabla} \times [\vec{\nabla} \times \hat{E}(\vec{r}, \omega)'] - \epsilon(\omega) \frac{\omega^2}{c^2} \hat{E}(\vec{r}, \omega)' = \frac{\omega^2}{\epsilon_0 c^2} \hat{P}(\vec{r}, \omega)' \quad (4.6)$$

and

$$\vec{\nabla} \times [\vec{\nabla} \times \bar{e}(\vec{r})] - \epsilon(\bar{\omega}) \frac{\bar{\omega}^2}{c^2} \bar{e}(\vec{r}) = \frac{\bar{\omega}^2}{\epsilon_0 c^2} \bar{p}(\vec{r}) \quad (4.7)$$

hold simultaneously. The last equation only contains the pump frequency, and its solution has to be matched across the boundaries $y = \pm L/2$ to the pump fields. The solution for $\bar{e}(\vec{r})$ can then be substituted into Eq. (4.2) to yield $\hat{P}^{(3)}$. In this fashion, the equations for the weak and the strong fields are decoupled, and $\hat{P}^{(3)}$ in Eq. (4.6) depends only parametrically on the pump fields. Since this will yield $\hat{P}^{(3)} \propto E'e^2$, the induced nonlinear polarization in the medium is proportional to the pump intensity, and such a medium is called a Kerr medium.

V. NONLINEAR POLARIZATION

As a slight approximation we shall use Kleinman's conjecture [31] for the elements of the susceptibility tensor. It states that these elements are invariant under a permutation of their arguments. Then we introduce the abbreviation

$$\chi = \hat{\chi}_{xyyy}^{(3)}(\bar{\omega}, \bar{\omega}, -\bar{\omega}). \quad (5.1)$$

We shall also assume that $\bar{\omega}$ is not too close to a resonance of the medium, which makes both χ and $\epsilon \equiv \epsilon(\bar{\omega})$

real.

Since the pumps are assumed to be linearly polarized in the z direction, we try a solution of the form

$$\vec{e}(\vec{r}) = \pi \vec{e}_z f(y), \quad -\infty < y < \infty, \quad (5.2)$$

which yields for the polarization in the medium

$$\vec{p}(\vec{r}) = \frac{3}{4} \chi \pi \epsilon_0 \vec{e}_z |f(y)|^2 f(y). \quad (5.3)$$

Then Eq. (4.7) reduces to

$$\left[\frac{d^2}{dy^2} + \bar{k}^2 [\epsilon + \frac{3}{4} \chi |f(y)|^2] \right] f(y) = 0, \quad (5.4)$$

and the boundary conditions at $y = \pm L/2$ are that f and df/dy must be continuous. A typical value of a third-order susceptibility is $\chi \sim 10^{-22} \text{ m}^2/\text{V}^2$ and a very strong laser has an electric-field strength of 10^{10} V/m . This gives $\chi |f|^2 \sim 0.01$. For moderate cw lasers or nanosecond pulses, values in the range of $\chi |f|^2 \sim 10^{-5} - 10^{-8}$ are more realistic. In any case, this parameter is always small compared to the dielectric constant and can therefore be neglected in Eq. (5.4). Then the problem reduces to the situation where two beams counterpropagate through a linear medium, and this can be solved in a straightforward way. With the phase convention (1.1) for the two pumps, the solution is found to be

$$f(y) = \alpha \bar{E} \cos(\bar{k}y \sqrt{\epsilon}), \quad (5.5)$$

with

$$\alpha = \frac{4e^{(1/2)i\bar{k}L(\sqrt{\epsilon}-1)}}{\sqrt{\epsilon}+1-(\sqrt{\epsilon}-1)e^{i\bar{k}L\sqrt{\epsilon}}}. \quad (5.6)$$

As shown below, the parameter α determines the strength of the nonlinear interaction. It depends on the optical wavelength, the dielectric constant, and the length L of the medium. By choosing L carefully, the strength of the interaction can be optimized.

Maxwell's equation (4.6) is a wave equation for $\hat{E}(\vec{r}, \omega)'$, which has $\hat{P}(\vec{r}, \omega)'$ as a source term. We shall assume that the incident field on the PC has a frequency distribution which is reasonably centered around $\pm\bar{\omega}$. The nonlinear interaction then couples the frequency bands around $\pm\bar{\omega}, \pm 3\bar{\omega}, \pm 5\bar{\omega}, \dots$, but there is no coupling to spectral components in between. Under the assumption that χ is very small when one of its frequency arguments is of the order of $\pm 3\bar{\omega}$, it then follows that the wave equations for $\omega \sim \pm\bar{\omega}$ decouple from the equations for the higher harmonics. This does not imply that there is no higher-harmonics generation due to the incident field and the pumps (the q terms), but only that these wave equations do not couple to the evolution of the radiation in the ranges around $\bar{\omega}$ and $-\bar{\omega}$. Then we substitute the solution for $\vec{e}(\vec{r})$ into expression (4.3) for \hat{P} and write out explicitly the "12 terms." With Eq. (4.5) we obtain for \hat{P}'

$$\hat{P}(\vec{r}, \omega)' = \begin{cases} \gamma_0 \epsilon_0 \mathcal{P} \{ 2\hat{E}(\vec{r}, \omega)' + e^{i\theta_p} \hat{E}(\vec{r}, \omega - 2\bar{\omega})' \} & \text{for } \omega \sim \bar{\omega}, \\ \gamma_0 \epsilon_0 \mathcal{P} \{ 2\hat{E}(\vec{r}, \omega)' + e^{-i\theta_p} \hat{E}(\vec{r}, \omega + 2\bar{\omega})' \} & \text{for } \omega \sim -\bar{\omega}, \end{cases} \quad (5.7)$$

where we have neglected terms that oscillate spatially with half an optical wavelength. The complex coupling parameter γ is defined as $\gamma = \frac{3}{8} \chi (\alpha \bar{E})^2$, which will be written as $\gamma = \gamma_0 \exp(i\theta_p)$, with $\gamma_0 = |\gamma| \text{sgn}(\chi)$ and θ_p real. The operator \mathcal{P} is defined by its action on an arbitrary vector \vec{v} according to

$$\mathcal{P}\vec{v} = \vec{v}_{\parallel} + 3\vec{v}_{\perp}, \quad (5.9)$$

where \vec{v}_{\parallel} and \vec{v}_{\perp} indicate the parallel and perpendicular parts of \vec{v} , respectively, with respect to the plane $z=0$. Operator \mathcal{P} accounts for the polarization of the pump beams, which we have chosen as the z direction. For other polarizations the form of this operator will be different, but the structure of Eqs. (5.7) and (5.8) remains essentially the same.

VI. COUPLED WAVE EQUATIONS

For the remainder of this paper we shall only be concerned with the weak fields, and therefore we drop the primes on \hat{E}' and \hat{P}' . Substituting expressions (5.7) and (5.8) into the wave equation (4.6) yields

$$\begin{aligned} \vec{\nabla} \times [\vec{\nabla} \times \hat{E}(\vec{r}, \omega)] - \frac{\omega^2}{c^2} (\epsilon + 2\gamma_0 \mathcal{P}) \hat{E}(\vec{r}, \omega) \\ = \frac{\omega^2}{c^2} \mathcal{P} \begin{cases} \gamma \hat{E}(\vec{r}, \omega - 2\bar{\omega}) & \text{for } \omega \sim \bar{\omega}, \\ \gamma^* \hat{E}(\vec{r}, \omega + 2\bar{\omega}) & \text{for } \omega \sim -\bar{\omega}. \end{cases} \end{aligned} \quad (6.1)$$

Suppose we have a given frequency $\omega_a > 0$, with $\omega_a \sim \bar{\omega}$. Then the first equation couples the field at ω_a to the field at $\omega_b = \omega_a - 2\bar{\omega}$ which is negative and around $-\bar{\omega}$. On the other hand, if we set $\omega = \omega_b$ in the second equation, then this spectral component couples to the field at ω_a . Hence the set (6.1) only couples frequencies in pairs. With Eq. (2.2) it follows that effectively ω_a couples to $-\omega_b$. It will turn out to be a computational advantage to work with the negative frequency ω_b rather than the positive frequency $-\omega_b$. Notice that ω_a and $-\omega_b$ are located symmetrically around the pump frequency $\bar{\omega}$. Therefore the electric field obeys the set of wave equations

$$\begin{aligned} \vec{\nabla} \times [\vec{\nabla} \times \hat{\vec{E}}(\vec{r}, \omega_a)] - \frac{\omega_a^2}{c^2} (\epsilon + 2\gamma_0 \mathcal{P}) \hat{\vec{E}}(\vec{r}, \omega_a) \\ = \gamma \frac{\omega_a^2}{c^2} \mathcal{P} \hat{\vec{E}}(\vec{r}, \omega_b), \end{aligned} \quad (6.2)$$

$$\begin{aligned} \vec{\nabla} \times [\vec{\nabla} \times \hat{\vec{E}}(\vec{r}, \omega_b)] - \frac{\omega_b^2}{c^2} (\epsilon + 2\gamma_0 \mathcal{P}) \hat{\vec{E}}(\vec{r}, \omega_b) \\ = \gamma^* \frac{\omega_b^2}{c^2} \mathcal{P} \hat{\vec{E}}(\vec{r}, \omega_b), \end{aligned} \quad (6.3)$$

for each pair (ω_a, ω_b) .

VII. DISPERSION RELATIONS

The coupled wave equations (6.2) and (6.3) admit plane-wave solutions of the form

$$\hat{\vec{E}}(\vec{r}, \omega_a) = E \vec{a} e^{i\vec{k} \cdot \vec{r}}, \quad \hat{\vec{E}}(\vec{r}, \omega_b) = E \vec{b} e^{i\vec{k} \cdot \vec{r}}, \quad (7.1)$$

with E arbitrary and vectors \vec{a} , \vec{b} , and \vec{k} to be determined. Both plane waves have the same wave vector \vec{k} . The ω_a wave propagates into the \vec{k} direction (for \vec{k} real), but the ω_b wave propagates into the opposite direction because ω_b is negative. Hence this solution consists of two counterpropagating waves with the same wavelength but different frequencies. Substitution of the ansatz (7.1) into (6.2) and (6.3) yields

$$\kappa^2 \vec{a} - (\vec{\kappa} \cdot \vec{a}) \vec{\kappa} - (\epsilon + 2\gamma_0 \mathcal{P}) \vec{a} = \gamma \mathcal{P} \vec{b}, \quad (7.2)$$

$$\kappa^2 \vec{b} - (\vec{\kappa} \cdot \vec{b}) \vec{\kappa} - \rho^2 (\epsilon + 2\gamma_0 \mathcal{P}) \vec{b} = \gamma^* \rho^2 \mathcal{P} \vec{a}, \quad (7.3)$$

where we have introduced the dimensionless wave vector $\vec{\kappa} = c\vec{k}/\omega_a$ and the frequency parameter $\rho = -\omega_b/\omega_a$. Due to the appearance of the operator \mathcal{P} , each of the vectors \vec{a} , \vec{b} , and $\vec{\kappa}$ separates into its parallel and perpendicular components with respect to the plane $z=0$. This implies that the set (7.2) and (7.3) is essentially a set of four equations with six unknowns. The requirement that the set has nontrivial solutions will then yield two restrictive relations. These are the dispersion relations for the wave vector $\vec{\kappa}$.

A. Transverse solution

In a linear medium, electromagnetic waves are transverse. It appears that also for the Kerr medium under consideration there are transverse solutions, e.g., solutions for which $\vec{\kappa} \cdot \vec{a} = \vec{\kappa} \cdot \vec{b} = 0$. From Eqs. (7.2) and (7.3) it then follows that $a_{\perp} = b_{\perp} = 0$, which implies that the polarization vectors \vec{a} and \vec{b} are parallel to the surface of the PC. Such waves are called surface polarized, or s polarized. The set of equations then reduces to a dispersion relation for the magnitude of the wave vector, $\kappa = |\vec{\kappa}|$, and the subscript s will indicate the solution for s waves. We obtain

$$[\kappa_s^2 - (\epsilon + 2\gamma_0)][\kappa_s^2 - \rho^2(\epsilon + 2\gamma_0)] - \gamma^2 \rho^2 = 0, \quad (7.4)$$

with solutions

$$\kappa_s^{(1)} = \left[\frac{1}{2} (\epsilon + 2\gamma_0) \left\{ \rho^2 + 1 \mp \delta \left[(\rho^2 - 1)^2 + \left(\frac{2\rho\gamma_0}{\epsilon + 2\gamma_0} \right)^2 \right]^{1/2} \right\} \right]^{1/2}, \quad (7.5)$$

where $\delta = \text{sgn}(\rho - 1)$. This gives the two branches $\kappa_s^{(1)}$ and $\kappa_s^{(2)}$ of the dispersion relation as a function of the frequency (parameter) ρ . Both solutions are shown in Fig. 2. We have chosen to define the branches with a discontinuity at the resonance frequency $\rho = 1$. In this way, we have $\kappa_s^{(1)} \rightarrow \sqrt{\epsilon}$ and $\kappa_s^{(2)} \rightarrow \rho\sqrt{\epsilon}$ for $\gamma_0 \rightarrow 0$, which are the dispersion relations for the ω_a wave and ω_b wave, respectively, in the absence of the nonlinear interaction.

B. Nontransverse solution

In a nonlinear medium, a traveling wave is not necessarily transverse. It appears that there exists a second class of solutions, in addition to the one above, for which the polarization vectors \vec{a} and \vec{b} are not perpendicular to the wave vector $\vec{\kappa}$. The vectors \vec{a} and \vec{b} lie in the plane through $\vec{\kappa}$ and \vec{e}_z , and therefore these waves are plane (p) polarized. Solving the set (7.2) and (7.3) for this situation yields the dispersion relation for these solutions. We find

$$\kappa_p^{(1)} = \left[\gamma_0 (2\epsilon + 9\gamma_0) y + \frac{1}{2} (\epsilon + 2\gamma_0) \left\{ \rho^2 + 1 \mp \delta \left[(\rho^2 - 1)^2 + \left(\frac{2\gamma_0}{\epsilon + 2\gamma_0} \right)^2 (1 + \epsilon y)(\rho^2 + \epsilon y) \right]^{1/2} \right\} \right]^{1/2}, \quad (7.6)$$

where we introduced the abbreviation

$$y = \frac{2\kappa_{\parallel}^2}{(\epsilon + 3\gamma_0)(\epsilon + 9\gamma_0)}. \quad (7.7)$$

This solution is very similar to (7.5), with the exception

that κ_p depends on κ_{\parallel} , the magnitude of $\vec{\kappa}_{\parallel}$. We shall take vector $\vec{\kappa}_{\parallel}$ as an independent parameter. If θ is the angle between $\vec{\kappa}$ and the z axis, then we have $\kappa_{\parallel} = \kappa \sin \theta$. Therefore κ_{\parallel} represents the propagation direction with respect to the z axis. It then follows that the dispersion relation for p waves depends on the direction of $\vec{\kappa}$, which makes

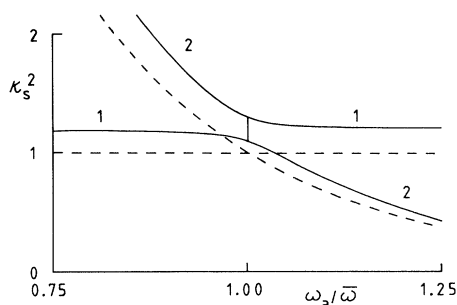


FIG. 2. This figure shows the two branches of the dispersion relation for s -polarized waves, as given by Eq. (7.5). Plotted is the square of the wave vector versus the frequency in units of the pump frequency, for $\epsilon=1$ and $\gamma_0=0.1$. The dashed lines indicate the corresponding relations for a dielectric ($\gamma_0=0$).

the medium effectively anisotropic. The material itself was assumed to be isotropic, but the polarization of the pumps destroys the symmetry. Since we took the pump polarization to be linear and in the z direction, the medium is still invariant for a rotation about the z axis. For $\kappa_{\parallel}=0$ the distinction between s and p waves disappears.

$$\eta_2 = \frac{2}{(\epsilon + 2\gamma_0)\{\rho^2 - 1 + \delta\sqrt{(\rho^2 - 1)^2 + [2\rho\gamma_0/(\epsilon + 2\gamma_0)]^2}\}}, \quad (8.6)$$

$$\eta_1 = -\rho^2 \eta_2. \quad (8.7)$$

The amplitude ratio of the ω_a wave and the ω_b wave is $|\gamma\eta_1|$ or $|\gamma\eta_2|$, and close to resonance ($\rho \approx 1$) this ratio approaches unity. In that case, both waves have equal intensity. For $\gamma \rightarrow 0$ (linear medium) or far off resonance, the ω_b wave in the first solution and the ω_a wave in the second solution disappear. Typical behavior of these parameters is illustrated in Fig. 3.

The polarization vectors for plane-polarized waves can

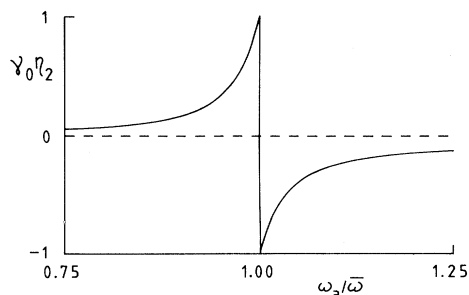


FIG. 3. Plot of $\gamma_0 \eta_2$ as a function of $\omega_a/\bar{\omega}$ for $\epsilon=1$ and $\gamma_0=0.1$. At resonance this parameter is discontinuous, with $|\gamma_0 \eta_2|=1$, and far off resonance it goes to zero.

VIII. AMPLITUDES OF THE COUPLED WAVES

Now that we have the solution for the wave vectors, given the frequency, we can solve the set (7.2) and (7.3) for the vectors \vec{a} and \vec{b} . For s waves, both vectors are parallel to the plane $z=0$, and Eqs. (7.2) and (7.3) reduce to

$$[\kappa_s^2 - (\epsilon + 2\gamma_0)]\vec{a} = \gamma\vec{b}, \quad (8.1)$$

$$[\kappa_s^2 - \rho^2(\epsilon + 2\gamma_0)]\vec{b} = \gamma^*\rho^2\vec{a}. \quad (8.2)$$

These equations are dependent by construction. Both \vec{a} and \vec{b} are perpendicular to both $\vec{\kappa}_{\parallel}$ and \vec{e}_z , and therefore proportional to the unit vector

$$\vec{e}_s = (\vec{\kappa}_{\parallel} \times \vec{e}_z) / \kappa_{\parallel}. \quad (8.3)$$

For the branch $\kappa_s^{(1)}$ of the dispersion relation we set

$$\vec{a}_{1s} = \vec{e}_s, \quad \vec{b}_{1s} = \gamma^*\eta_1\vec{e}_s, \quad (8.4)$$

and for $\kappa_s^{(2)}$ we take

$$\vec{a}_{2s} = \gamma\eta_2\vec{e}_s, \quad \vec{b}_{2s} = \vec{e}_s. \quad (8.5)$$

Substitution into Eq. (8.1) or (8.2) then gives

be found along similar lines, although the computations are more involved. The vectors \vec{a} and \vec{b} lie in a plane through \vec{e}_z and $\vec{\kappa}_{\parallel}$, and can therefore be written as

$$\vec{a}_{ip} = \alpha_{i1}\vec{e}_z + \alpha_{i\parallel}\vec{\kappa}_{\parallel}/\kappa_{\parallel}, \quad (8.8)$$

$$\vec{b}_{ip} = \beta_{i1}\vec{e}_z + \beta_{i\parallel}\vec{\kappa}_{\parallel}/\kappa_{\parallel}, \quad (8.9)$$

with $i=1$ or 2 , corresponding to the two branches of the dispersion relation. We choose the parameters such that for $\gamma \rightarrow 0$ or far off resonance the ω_b wave disappears for $i=1$ and the ω_a wave for $i=2$. The other two vectors will be normalized as

$$\vec{a}_{1p} \cdot \vec{a}_{1p} = 1, \quad \vec{b}_{2p} \cdot \vec{b}_{2p} = 1, \quad (8.10)$$

just as for s waves. The α and β parameters are fairly complicated, and listed in Appendix A.

IX. INCIDENT FIELD

Two counterpropagating waves $\hat{E}(\vec{r}, \omega_a)$ and $\hat{E}(\vec{r}, \omega_b)$ inside the medium have the appearance of a plane wave and its phase-conjugate image, apart from a slight frequency shift. When a plane wave with frequency ω_a is incident upon the medium from the region $z > 0$, then this

wave will (partially) propagate into the medium and, due to the nonlinear interaction, couple to the corresponding ω_b wave. This field will exit the medium again and travel into the positive- z direction, counterpropagating the incident wave. In this fashion, a phase-conjugate replica of the incident field is generated. In the remainder of this paper we shall study this process in detail.

The incident field is assumed to be a monochromatic polarized plane wave of the form

$$\hat{\vec{E}}(\vec{r}, \omega_a)_{\text{inc}} = E \vec{e}_\sigma e^{i\vec{k} \cdot \vec{r}}, \quad (9.1)$$

with $\sigma = s$ or p , $k = \omega_a/c$, and $\vec{k} \cdot \vec{e}_\sigma = 0$. Given k (or ω_a) and k_\parallel , the z component of \vec{k} is determined up to a minus sign. The sign must be chosen such that for a traveling wave the propagation direction is in the negative- z direction, and for an evanescent wave the amplitude must decrease exponentially into this direction. Therefore we must take

$$k_z = \begin{cases} -\sqrt{k^2 - k_\parallel^2}, \\ -i\sqrt{k_\parallel^2 - k^2}, \end{cases} \quad (9.2)$$

and we use the value for which the argument of the square root is positive. Then we let $\bar{\kappa}_\parallel = k_\parallel/k$. For $0 \leq \bar{\kappa}_\parallel < 1$ we have a traveling incident wave and $\sin\theta_i = \bar{\kappa}_\parallel$, with θ_i the angle of incidence. For $\bar{\kappa}_\parallel > 1$ the wave is evanescent. The dimensionless z component is defined by $\kappa_a = k_z/k$, which is explicitly

$$\kappa_a = \begin{cases} -\sqrt{1 - \bar{\kappa}_\parallel^2}, \\ -i\sqrt{\bar{\kappa}_\parallel^2 - 1}. \end{cases} \quad (9.3)$$

X. SET OF COUPLED WAVES

The incident wave couples to other waves inside and outside the medium, in a way which is determined by the boundary conditions at $z=0$ and $z=-\Delta$. Each plane wave will have an \vec{r} dependence of the form $\exp(i\vec{k}_i \cdot \vec{r})$. At $z=0$ this reduces to $\exp(i\bar{\kappa}_{i,\parallel} \vec{r})$, and it is easy to see that the boundary conditions can only be satisfied if this factor cancels out. This implies that each wave vector must have the same parallel component, which is equal to $\bar{\kappa}_\parallel$ of the incident wave. The magnitude of each wave vector is determined by the dispersion relation, either in the medium or in vacuum, and this fixes the z component of each wave vector, apart from its sign.

In the region $z > 0$ the incident wave with frequency ω_a can couple to a specular wave at the same frequency, just as in linear optics. Since the incident wave vector equals $\vec{k} = k(\bar{\kappa}_\parallel + \kappa_a \vec{e}_z)$, the specular wave must have wave vector

$$\vec{k}_r = k(\bar{\kappa}_\parallel - \kappa_a \vec{e}_z). \quad (10.1)$$

We shall call this the r wave. At frequency ω_b the dispersion relation is $k_t = \omega_b/c$, which admits two solutions for the z component of the wave vector. However, this wave

emanates from the medium, and only the causal solution is acceptable. This wave is the phase-conjugate image of the incident field, called the pc wave. The wave vector is

$$\vec{k}_{\text{pc}} = k(\bar{\kappa}_\parallel + \kappa_b \vec{e}_z), \quad (10.2)$$

with

$$\kappa_b = \begin{cases} -\sqrt{\rho^2 - \bar{\kappa}_\parallel^2}, \\ i\sqrt{\bar{\kappa}_\parallel^2 - \rho^2}. \end{cases} \quad (10.3)$$

Recall that ω_b is negative, which means that this wave travels in the direction opposite to its wave vector. The various wave vectors are shown in Fig. 4 for traveling waves and in Fig. 5 for evanescent waves. Due to the small difference between ω_a and ω_b , the wave vector of the pc wave is not exactly parallel to the incident wave vector and the wavelength is also slightly different.

The region $z < -\Delta$ is also vacuum, and this allows four different waves, given $\bar{\kappa}_\parallel$. However, only two of them are causal. The ω_a wave which travels or decays in the negative- z direction is the transmitted (t) wave with wave vector $\vec{k}_t = \vec{k}$. The possible ω_b wave, called the nonlinear (nl) wave, must have wave vector

$$\vec{k}_{\text{nl}} = k(\bar{\kappa}_\parallel - \kappa_b \vec{e}_z). \quad (10.4)$$

As seen in Fig. 4, this wave travels in the direction opposite to the specular wave. This wave is generated by the nonlinear interaction, and disappears in the limit $\gamma \rightarrow 0$ (as does the pc wave).

For a given polarization $\sigma = s$ or p and a given $\bar{\kappa}_\parallel$, the dispersion relation inside the medium has two branches, labeled (1) and (2), and for each of these the z component of the wave vector can have two values which differ by a minus sign. Therefore the four possible wave vectors are

$$\vec{k}_{1\sigma}^\pm = k(\bar{\kappa}_\parallel \pm \kappa_{\alpha\sigma} \vec{e}_z), \quad (10.5)$$

$$\vec{k}_{2\sigma}^\pm = k(\bar{\kappa}_\parallel \pm \kappa_{\beta\sigma} \vec{e}_z), \quad (10.6)$$

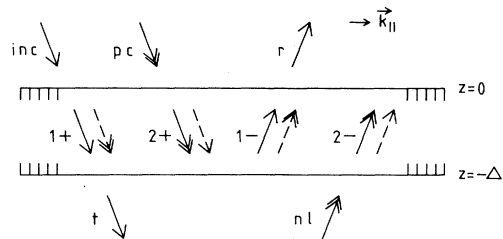


FIG. 4. Schematic representation of the various traveling waves which can be excited simultaneously by the incident field. The solid arrows indicate a principal wave, which can either be an ω_a wave (for $1\pm$) or an ω_b wave (for $2\pm$), and the broken arrows represent the waves which are coupled to the principal waves via the nonlinear interaction. A double arrowhead indicates a wave vector of an ω_b wave, which travel into the direction opposite the wave vector (because ω_b is negative).

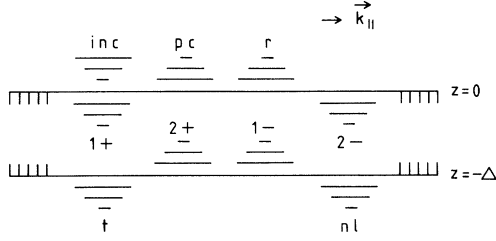


FIG. 5. Same as Fig. 4 but for evanescent waves. The ω_a waves travel into the direction of \vec{k}_{\parallel} , whereas the ω_b waves travel to the left. Two waves in a pair travel in opposite directions but decay in the same direction.

in terms of the dimensionless wave numbers

$$\kappa_{a\sigma} = \begin{cases} -\sqrt{(\kappa_{\sigma}^{(1)})^2 - \kappa_{\parallel}^2}, \\ -i\sqrt{\kappa_{\parallel}^2 - (\kappa_{\sigma}^{(1)})^2}, \end{cases} \quad (10.7)$$

$$\kappa_{b\sigma} = \begin{cases} -\sqrt{(\kappa_{\sigma}^{(2)})^2 - \kappa_{\parallel}^2}, \\ i\sqrt{\kappa_{\parallel}^2 - (\kappa_{\sigma}^{(2)})^2}. \end{cases} \quad (10.8)$$

Since each of the four wave vectors represents a pair of coupled waves, there are eight different waves possible inside the medium, as illustrated in Fig. 4. There is no causality requirement in a layer with finite thickness, and therefore all possible solutions for the dispersion relation will contribute. The boundary conditions then couple all 13 waves shown in Fig. 4 or Fig. 5.

XI. THE FIELDS

All waves have a spatial dependence of the form $\exp(i\vec{k}_i \cdot \vec{r})$, with the wave vectors \vec{k}_i given in the previous section. Next we have to choose a phase convention for the polarization vectors. In vacuum we take for s waves

$$\vec{e}_{s,i} = (\vec{\kappa}_{\parallel} \times \vec{e}_z) / \kappa_{\parallel}, \quad (11.1)$$

as in Eq. (8.3), and for p -polarized waves we take

$$\vec{e}_{p,i} = (\vec{k}_i \times \vec{e}_s) / k_i. \quad (11.2)$$

Both vectors are unit vectors, and are perpendicular to the corresponding wave vector. We note that $\vec{e}_{p,i}$ is complex for evanescent waves. The field in the region $z > 0$ then attains the form

$$\hat{\vec{E}}(\vec{r}, \omega_a) = E \{ \vec{e}_{\sigma} e^{i\vec{k} \cdot \vec{r}} + R_{\sigma} \vec{e}_{\sigma,r} e^{i\vec{k}_r \cdot \vec{r}} \}, \quad (11.3)$$

$$\hat{\vec{E}}(\vec{r}, \omega_b) = EP_{\sigma} \vec{e}_{\sigma,pc} e^{i\vec{k}_{pc} \cdot \vec{r}}, \quad (11.4)$$

representing the incident wave, the specular wave, and the phase-conjugated wave. The factor E is common for all waves. The relative strength of the various waves with respect to the incident wave is given by the Fresnel coefficients R_{σ} and P_{σ} . These will be determined by imposing the boundary conditions. Similarly, in the region

$z < -\Delta$ the field has the form

$$\hat{\vec{E}}(\vec{r}, \omega_a) = ET_{\sigma} \vec{e}_{\sigma,t} e^{i\vec{k}_t \cdot \vec{r}}, \quad (11.5)$$

$$\hat{\vec{E}}(\vec{r}, \omega_b) = EN_{\sigma} \vec{e}_{\sigma,nl} e^{i\vec{k}_{nl} \cdot \vec{r}}, \quad (11.6)$$

with T_{σ} and N_{σ} to be determined.

Inside the medium we have eight waves, and their polarization vectors were determined in Sec. VIII. It was shown that the relative strength of two waves in a pair is determined by the dispersion relation, and therefore not by boundary conditions. Hence a Fresnel coefficient for a pair of coupled waves determines the relative intensity of the pair with respect to the incident wave. Explicitly, the field is

$$\hat{\vec{E}}(\vec{r}, \omega_a) = E \left\{ Z_{\sigma}^{1+} a_{\sigma}^{1+} e^{i\vec{k}_{\sigma}^{1+} \cdot \vec{r}} + Z_{\sigma}^{1-} a_{\sigma}^{1-} e^{i\vec{k}_{\sigma}^{1-} \cdot \vec{r}} \right. \\ \left. + Z_{\sigma}^{2+} a_{\sigma}^{2+} e^{i\vec{k}_{\sigma}^{2+} \cdot \vec{r}} + Z_{\sigma}^{2-} a_{\sigma}^{2-} e^{i\vec{k}_{\sigma}^{2-} \cdot \vec{r}} \right\}, \quad (11.7)$$

$$\hat{\vec{E}}(\vec{r}, \omega_b) = E \left\{ Z_{\sigma}^{1+} b_{\sigma}^{1+} e^{i\vec{k}_{\sigma}^{1+} \cdot \vec{r}} + Z_{\sigma}^{1-} b_{\sigma}^{1-} e^{i\vec{k}_{\sigma}^{1-} \cdot \vec{r}} \right. \\ \left. + Z_{\sigma}^{2+} b_{\sigma}^{2+} e^{i\vec{k}_{\sigma}^{2+} \cdot \vec{r}} + Z_{\sigma}^{2-} b_{\sigma}^{2-} e^{i\vec{k}_{\sigma}^{2-} \cdot \vec{r}} \right\}, \quad (11.8)$$

with the four Fresnel coefficients $Z_{\sigma}^{\pm\pm}$ to be determined.

XII. FRESNEL COEFFICIENTS

Maxwell's equations require that at the boundaries $z=0$ and $z=-\Delta$ the fields $\hat{\vec{E}}_{\parallel}$, $\hat{\vec{B}}$, and $(\epsilon \hat{\vec{E}} + \hat{\vec{P}} / \epsilon_0)_{\perp}$ are continuous, for both ω_a and ω_b . This yields two sets (one for each value of σ) of 12 linear equations for the eight unknown Fresnel coefficients, which shows that the sets are overdetermined. If we consider the continuity of $\hat{\vec{E}}_{\parallel}$ and $\hat{\vec{B}}$ only, then we have two sets of eight equations with eight unknowns. It can be shown that then also $(\epsilon \hat{\vec{E}} + \hat{\vec{P}} / \epsilon_0)_{\perp}$ is continuous at both boundaries. For s waves this is obvious, because all fields are parallel to the surface so that $(\epsilon \hat{\vec{E}} + \hat{\vec{P}} / \epsilon_0)_{\perp} = 0$. For p waves the third boundary condition yields a set of equations which is identical to the set that is derived from the continuity of the magnetic field.

For each $\hat{\vec{E}}$ field the corresponding magnetic field is found with Eq. (2.4). After writing out the first two boundary conditions it follows that each set of eight equations separates into two sets of four equations. The Fresnel coefficients for the waves inside the medium follow from the solution of

$$F_\sigma \begin{bmatrix} Z_\sigma^{1+} \\ Z_\sigma^{1-} \\ Z_\sigma^{2+} \\ Z_\sigma^{2-} \end{bmatrix} = \begin{bmatrix} 2\kappa_a \\ 0 \\ 0 \\ 0 \end{bmatrix}, \quad (12.1)$$

with F_σ 4×4 matrices, which are given explicitly in Appendix B (one for each σ). After that, the remaining Fresnel coefficients are found from the solution of

$$\begin{bmatrix} R_\sigma \\ P_\sigma \\ T_\sigma e^{-i\phi_a} \\ N_\sigma e^{i\phi_b} \end{bmatrix} = \begin{bmatrix} -1 \\ 0 \\ 0 \\ 0 \end{bmatrix} + G_\sigma \begin{bmatrix} Z_\sigma^{1+} \\ Z_\sigma^{1-} \\ Z_\sigma^{2+} \\ Z_\sigma^{2-} \end{bmatrix}, \quad (12.2)$$

with the matrices G_σ given in Appendix B. The phases are defined as $\phi_i = 2\pi\kappa_i d$ for each wave number κ_i ($i = a, b, \alpha\sigma$, or $\beta\sigma$), and $d = k\Delta/2\pi$ is the layer thickness, measured in wavelengths of the incident field. Solving Eq. (12.1) requires the inversion of the 4×4 matrices, whereas Eq. (12.2) is a simple matrix product. The equations can be solved analytically, but the resulting expressions are awkward and will not be given here. The illustrations below are numerical solutions.

XIII. RESONANCE IN A TRANSPARENT MEDIUM

The nonlinear interaction enters the equations for the Fresnel coefficients through the parameter γ , which is always very small compared to unity. In what follows we take γ_0 to be positive, in order to simplify the notation a little. Since γ_0 is so small, it is tempting to simplify expressions like (8.6) for η_2 by letting $\gamma_0 \rightarrow 0$. Care should be exercised, however, in this procedure. For instance, for $\gamma_0 \rightarrow 0$ the expression for η_2 reduces to

$$\eta_2 = \frac{1}{\epsilon(\rho^2 - 1)}, \quad (13.1)$$

whereas close to resonance ($\omega_a \rightarrow \bar{\omega}$, or $\rho \rightarrow 1$) we have

$$\eta_2 = \delta/\gamma_0. \quad (13.2)$$

This shows that near resonance $\gamma_0\eta_2$ remains finite, and Eq. (13.1) does not give the correct behavior. Therefore, the resonance condition is $|\rho - 1| \ll \gamma_0$, and we could call γ_0 the bandwidth of the PC as a function of ρ . As a function of ω the bandwidth is then $\gamma_0\bar{\omega}/2$, which is of the order of 10 MHz–10 GHz. It is easy to show that for $|\rho - 1| \gg \gamma_0$ all ω_b waves disappear, and the remaining Fresnel coefficients are the Fresnel coefficients for a dielectric layer.

In this section we consider the limit $\rho \rightarrow 1$, $\gamma_0 \rightarrow 0$, but such that $|\rho - 1| \ll \gamma_0$. We shall assume that all waves are traveling waves and that the medium is transparent ($\epsilon = 1$). Then the wave numbers which appear in the matrices of Appendix B become

$$\kappa_a = \kappa_b = \kappa_{\alpha\sigma} = \kappa_{\beta\sigma} = -\cos\theta_i, \quad (13.3)$$

with θ_i the angle of incidence. The q parameters for the

p waves simplify to

$$q_1 = \bar{q}_1 = q_4 = \bar{q}_4 = 1, \quad (13.4)$$

$$q_2 = \bar{q}_2 = -q_3 = -\bar{q}_3 = -\delta/\gamma_0, \quad (13.5)$$

and the matrices for p polarization are identical in form to the matrices for s polarization. The solution is then easily found to be

$$Z_\sigma^{1-} = Z_\sigma^{2-} = R_\sigma = N_\sigma = 0, \quad (13.6)$$

$$Z_\sigma^{1+} = \frac{1}{2} \frac{1 + e^{i\phi_\sigma}}{1 + \cos\phi_\sigma}, \quad (13.7)$$

$$Z_\sigma^{2+} = \delta e^{-i\theta_p} (Z_\sigma^{1+})^*, \quad (13.8)$$

$$P_\sigma = -i\delta e^{-i\theta_p} \tan\{\frac{1}{2}\phi_\sigma\}, \quad (13.9)$$

$$T_\sigma = e^{i(\phi_a - \phi_{\alpha\sigma})} \frac{1 + e^{i\phi_\sigma}}{1 + \cos\phi_\sigma}, \quad (13.10)$$

where we have set $\phi_\sigma = \phi_{\alpha\sigma} - \phi_{\beta\sigma}$. Equation (13.6) expresses that all the waves on the right-hand side in Fig. 4, which are associated with the specular wave, disappear in a transparent medium. The remaining Fresnel coefficients are determined by the phases $\phi_{\alpha\sigma} = 2\pi d\kappa_{\alpha\sigma}$ and $\phi_{\beta\sigma} = 2\pi d\kappa_{\beta\sigma}$ (and the phase θ_p of γ). According to Eq. (13.3) we have $\kappa_{\alpha\sigma} = \kappa_{\beta\sigma}$, which seems to make both phases equal. With Eq. (13.9) this would give $P_\sigma = 0$, so that there would not be any phase-conjugated wave. However, the wave numbers are multiplied by the dimensionless layer thickness d , which is large. For Δ a few centimeters we have $d \sim 10^5$. Both wave numbers are equal in the limit $\gamma_0 \rightarrow 0$, but this means that their difference is of the order of γ_0 . Multiplied by d , this can yield any value for $\phi_{\alpha\sigma} - \phi_{\beta\sigma}$. This also implies that a sufficient layer thickness (interaction length) is required in order for the medium to generate a phase-conjugated signal. This has been known for a long time [32,33]. At resonance, the two waves in a pair have equal strength, as shown in Sec. VIII, and with Eq. (13.8) we find that $|Z_\sigma^{1+}| = |Z_\sigma^{2+}|$. This gives all four waves in the medium equal intensity.

The dependence on the angle of incidence is contained in ϕ_σ , and we have to lowest order in γ_0

$$\phi_s = \delta \frac{2\pi d \gamma_0}{\cos\theta_i}, \quad (13.11)$$

$$\phi_p = \delta \frac{2\pi d \gamma_0}{\cos\theta_i} (1 + 2 \sin^2\theta_i). \quad (13.12)$$

Both phases are proportional to $\delta = \text{sgn}(\rho - 1)$, and so this δ cancels the δ in Eq. (13.9). Therefore there is no discontinuity in the phase of P_σ at resonance. For $\theta_i \rightarrow 90^\circ$ we have $\cos\theta_i \rightarrow 0$ which makes the phases ϕ_σ grow very rapidly, and consequently P_σ oscillates very rapidly. This feature is illustrated in Fig. 6. From Eq. (13.9) it follows that P_σ lies in the range $0 \leq |P_\sigma| < \infty$, and $|P_\sigma|$ can easily exceed unity, as is also evident in Fig. 6. This corresponds to amplification of the phase-conjugated wave with respect to the incident wave.

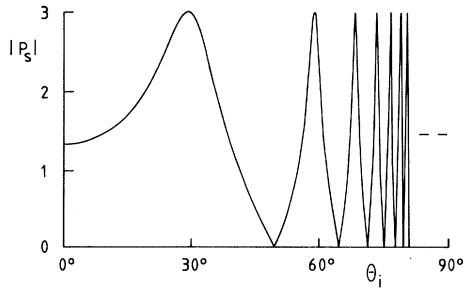


FIG. 6. Absolute value of P_s as a function of the angle of incidence, for $|\rho-1|=2\times 10^{-4}$, $\gamma=6\times 10^{-4}$, $\epsilon=1$, and $d=2083$. The value of ρ is such that the frequency is close to resonance. The maxima are located at 34° , 60° , 74° , 77° , 79° , 80° , ... as can be calculated from Eqs. (13.9) and (13.11). Due to the fact that γ_0 is finite, the peak heights remain also finite.

Values of $|P_\sigma|$ far above unity are called self-oscillation, and this has been observed experimentally [32]. The energy for amplification is, of course, provided by the pumps, and this leads to pump depletion. This effect is not taken into account here. From Eq. (13.10) it follows that the Fresnel coefficient for the transmitted wave is in the range $1 \leq |T_\sigma| < \infty$, which shows that the transmitted wave is always amplified as compared to the incident wave. The intensities of the fields are proportional to the squares of the absolute values of the Fresnel coefficients, and we have

$$|P_\sigma|^2 = \tan^2(\phi_\sigma/2), \quad |T_\sigma|^2 = \sec^2(\phi_\sigma/2), \quad (13.13)$$

from which it follows that

$$|T_\sigma|^2 - |P_\sigma|^2 = 1, \quad (13.14)$$

for any angle of incidence. It also follows immediately that

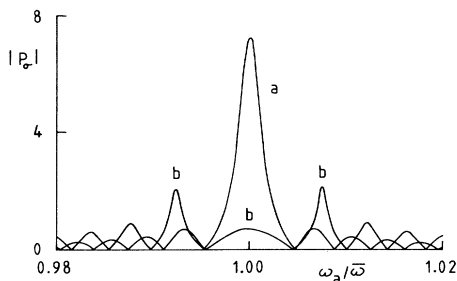


FIG. 7. Curves a and b represent $|P_s|$ and $|P_p|$, respectively, as a function of $\omega_a/\bar{\omega}$. The parameters are $\epsilon=1$, $\gamma=0.01$, $d=105$, and $\kappa_{\parallel}=1/\sqrt{2}$. The peak heights are different for s and p waves, and the maxima appear at different frequencies. The peak at resonance for p waves is weaker than two of the sidebands.

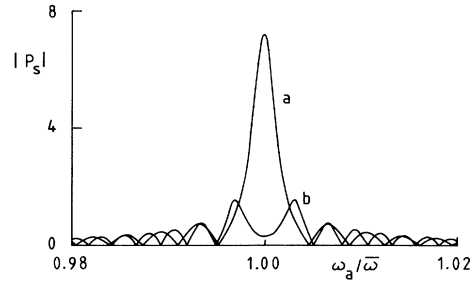


FIG. 8. Plot of $|P_s|$ versus $\omega_a/\bar{\omega}$ for two values of the layer thickness d . Curves a and b correspond to $d=105$ and $d=150$, respectively, and the other parameters are $\epsilon=1$, $\gamma=0.01$, and $\kappa_{\parallel}=1/\sqrt{2}$. Curve b shows that $|P_s|$ can have a minimum at resonance.

$$|T_\sigma|^2 = 4|Z_\sigma^{1+}|^2, \quad (13.15)$$

showing that the total intensity of the four waves in the medium equals the intensity of the transmitted wave.

XIV. RESULTS

When the incident wave is not in perfect resonance with the pumps, then the expressions from the previous section do not hold anymore. For a transparent medium it is still possible to derive good approximations because Eq. (13.6) holds. For instance, the reflection coefficient for s waves becomes

$$P_s = \gamma^* \eta_2 \frac{1 - e^{i(\phi_{as} - \phi_{bs})}}{\gamma_0^2 \eta_2^2 + e^{i(\phi_{as} - \phi_{bs})}}, \quad (14.1)$$

with η_2 given by Eq. (8.6). Similar expressions can be derived for the other Fresnel coefficients. The frequency dependence is contained in the parameter η_2 , as shown in Fig. 3, and in a more complicated way in the phase

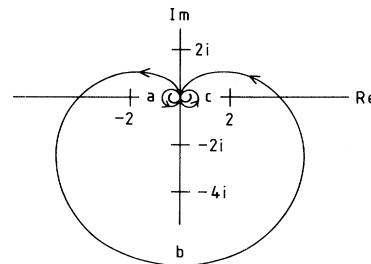


FIG. 9. Polar plot of P_s as a function of $\omega_a/\bar{\omega}$ in the complex plane, and for the same parameters as in Fig. 7. The arrowheads indicate the direction of increasing frequency, and points a , b , and c correspond to $\omega_a/\bar{\omega}=0.993$, 1.000 , and 1.007 , respectively. These points correspond to the central peak and the two sidebands in Fig. 7. The polar angle equals the phase shift upon reflection.

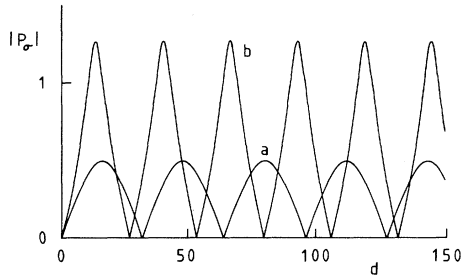


FIG. 10. Curves *a* and *b* give $|P_s|$ and $|P_p|$, respectively, as a function of the layer thickness d . The parameters are taken to be $\omega_a/\bar{\omega}=1.01$, $\epsilon=1$, $\gamma=0.01$, and $\theta_i=45^\circ$. The peaks appear to be equidistant, as they should according to Eqs. (13.9), (13.11), and (13.12).

$\phi_{\alpha s} - \phi_{\beta s}$. Equation (14.1) predicts that the peak values of $|P_s|$ are approximately 3.0 for the parameters in Fig. 6, which is seen to be very accurate. The frequency dependence of $|P_s|$ and $|P_p|$ is illustrated in Figs. 7 and 8. In most cases, $|P_\sigma|$ will have a pronounced maximum at resonance, and this allows the PC to act as a narrow optical bandpass filter, as was first realized by Pepper and Abrams [34]. The Fresnel coefficients appear to have many side peaks, which are a result of the ρ dependence of $\phi_{\alpha\sigma}$ and $\phi_{\beta\sigma}$. For some parameters there can even be a minimum at resonance, as shown in Fig. 8, and this was indeed observed experimentally [35]. Figure 9 shows a polar diagram of P_s in the complex plane, and it is seen that the phase changes with the frequency. This behavior is entirely geometrical because the frequency dependence of the susceptibility is only parametric. This result has been found before [36]. It can be shown that Eq. (13.14) also holds off resonance, provided that the medium is transparent.

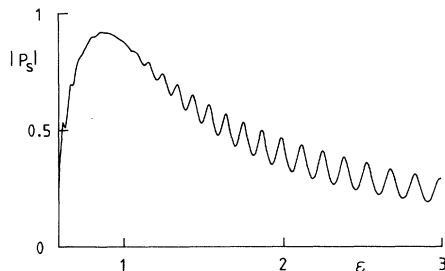


FIG. 11. Plot of $|P_s|$ versus the dielectric constant ϵ , for $\omega_a/\bar{\omega}=0.985$, $\gamma=0.03$, $d=10$, and $\kappa_{\parallel}=1/\sqrt{2}$. The maximum phase-conjugate reflectivity occurs around $\epsilon=1$. For larger values of ϵ the reflectivity decreases rapidly, and in an oscillatory way. At $\epsilon=0.5$ we have $\epsilon=\kappa_{\parallel}^2$, which implies $\kappa_{\alpha s}=\kappa_{\beta s}=0$. At this point the waves inside the medium become evanescent, and the phase-conjugate signal disappears.

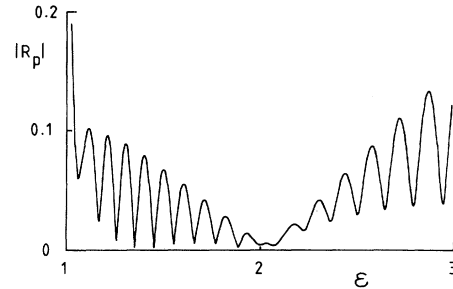


FIG. 12. Plot of the reflection coefficient $|R_p|$ as a function of the dielectric constant, and for $\omega_a/\bar{\omega}=0.985$, $\gamma=0.05$, $d=10$, and $\kappa_{\parallel}=0.819$ ($\theta_i=55^\circ$). For $\epsilon=1$ the reflectivity is not identically zero, which is due to the nonlinear interaction ($\gamma \neq 0$). Similarly, at $\epsilon=2$ we have $\epsilon=\tan^2\theta_i$, so that θ_i equals the Brewster angle. The linear interaction would then give $R_p \equiv 0$, but for $\gamma \neq 0$ there is a residual reflection into the specular direction.

In Fig. 10 the dependence of the reflection coefficients $|P_\sigma|$ on the layer thickness d is shown. This oscillatory behavior is very similar as for reflection at an ordinary dielectric. Finally, Figs. 11 and 12 illustrate the dependence on the dielectric constant. In most cases, the values of $|P_\sigma|$ are maximum around $\epsilon=1$. The dependence on ϵ follows from the general solution of Eqs. (12.1) and (12.2), and for $\epsilon \neq 1$ also the specular wave will appear, and the nl wave, and four more waves inside the medium. The appearance of the r wave is illustrated in Fig. 12.

XV. CONCLUSIONS

We have studied optical phase conjugation by four-wave mixing in a nonlinear medium, without restrictions on the angle of incidence, the value of the dielectric constant, and the frequency mismatch between the incident field and the pumps, and we did not use the slowly varying amplitude approximation. This led to dispersion relations for s waves and p waves and to the set of equations (12.1) and (12.2) for the Fresnel coefficients of the 13 plane waves that couple together. Inside the medium, waves always couple in pairs of counterpropagating waves. It appeared that the s waves are transverse, but the p waves are not. For a transparent medium in combination with resonance, the results for $|P_\sigma|^2$ and $|T_\sigma|^2$ simplify to their form in Eq. (13.13), and these expressions were found before [2,32]. Also included is the possibility that some of the waves are evanescent rather than traveling. The role of evanescent waves in optical phase conjugation has been studied recently in more detail [37,38]. The polarization properties in phase conjugation were also studied in Ref. [39], in a slightly different way, and in Ref. [40] the effect of nonuniform pump beams was investigated.

If the incident wave has a frequency ω_a , then its phase-conjugate image has a frequency of $\omega'_a = \rho\omega_a$ (which is $-\omega_b$), and both waves nearly counterpro-

pagate. This leads to interference fringes, which have been observed experimentally [36,41]. The angle of incidence θ_i is determined by the wave vector according to $\sin\theta_i = \kappa_{\parallel}$. With θ_{pc} the angle between the propagation direction of the pc wave and the normal to the surface $z=0$, we have $\sin\theta_{pc} = \kappa_{\parallel}/\rho$. Therefore the two angles are related by

$$\omega_a \sin\theta_i = \omega'_a \sin\theta_{pc}, \quad (15.1)$$

or $\sin\theta_i = \rho \sin\theta_{pc}$. The angle of reflection of the r wave is, of course, θ_i .

APPENDIX A

The α and β parameters for the polarization vectors of p waves can be expressed in terms of the auxiliary parameters

$$\xi_1 = \frac{3\rho^2(\varepsilon + \gamma_0)(\varepsilon + 3\gamma_0) - 2\varepsilon[(\kappa_p^{(1)})^2 - \kappa_{\parallel}^2]}{[(\kappa_p^{(1)})^2 - \rho^2(\varepsilon + 6\gamma_0)](\varepsilon + \gamma_0)(\varepsilon + 3\gamma_0) + 2\gamma_0(2\varepsilon + 3\gamma_0)[(\kappa_p^{(1)})^2 - \kappa_{\parallel}^2]}, \quad (A1)$$

$$\xi_2 = \frac{3(\varepsilon + \gamma_0)(\varepsilon + 3\gamma_0) - 2\varepsilon[(\kappa_p^{(2)})^2 - \kappa_{\parallel}^2]}{[(\kappa_p^{(2)})^2 - (\varepsilon + 6\gamma_0)](\varepsilon + \gamma_0)(\varepsilon + 3\gamma_0) + 2\gamma_0(2\varepsilon + 3\gamma_0)[(\kappa_p^{(2)})^2 - \kappa_{\parallel}^2]}, \quad (A2)$$

which contain the two solutions of the dispersion relation. We then obtain

$$\alpha_{1\perp} = \frac{-\kappa_{\parallel}}{\sqrt{\kappa_{\parallel}^2 + \{\kappa_{\parallel}^2 - (\varepsilon + 6\gamma_0) - 3\gamma_0^2\xi_1\}^2 / [(\kappa_p^{(1)})^2 - \kappa_{\parallel}^2]}}, \quad (A3)$$

$$\beta_{2\perp} = \frac{-\kappa_{\parallel}}{\sqrt{\kappa_{\parallel}^2 + \{\kappa_{\parallel}^2 - \rho^2(\varepsilon + 6\gamma_0) - 3\gamma_0^2\rho^2\xi_2\}^2 / [(\kappa_p^{(2)})^2 - \kappa_{\parallel}^2]}}, \quad (A4)$$

$$\beta_{1\perp} = \gamma^* \xi_1 \alpha_{1\perp}, \quad (A5)$$

$$\alpha_{2\perp} = \gamma \xi_2 \beta_{2\perp}. \quad (A6)$$

For the parallel components we find

$$\alpha_{1\parallel} = \frac{\alpha_{1\perp}}{\kappa_{\parallel} \kappa_{p,\perp}^{(1)}} \{ \kappa_{\parallel}^2 - (\varepsilon + 6\gamma_0) - 3\gamma_0^2 \xi_1 \}, \quad (A7)$$

$$\beta_{1\parallel} = \gamma^* \frac{\alpha_{1\perp}}{\kappa_{\parallel} \kappa_{p,\perp}^{(1)}} \{ \xi_1 [\kappa_{\parallel}^2 - \rho^2(\varepsilon + 6\gamma_0)] - 3\rho^2 \}, \quad (A8)$$

$$\alpha_{2\parallel} = \gamma \frac{\beta_{2\perp}}{\kappa_{\parallel} \kappa_{p,\perp}^{(2)}} \{ \xi_2 [\kappa_{\parallel}^2 - (\varepsilon + 6\gamma_0)] - 3 \}, \quad (A9)$$

$$\beta_{2\parallel} = \frac{\beta_{2\perp}}{\kappa_{\parallel} \kappa_{p,\perp}^{(2)}} \{ \kappa_{\parallel}^2 - \rho^2(\varepsilon + 6\gamma_0) - 3\gamma_0^2 \rho^2 \xi_2 \}. \quad (A10)$$

The quantity $\kappa_{p,\perp}$ follows from the dispersion relation according to $\kappa_{p,\perp} = \pm \{ \kappa_p^2 - \kappa_{\parallel}^2 \}^{1/2}$. Due to the \pm sign there are two solutions which differ in their propagation direction with respect to the z axis.

APPENDIX B

The two matrices which determine the Fresnel coefficients for s waves are found to be

$$F_s = \begin{bmatrix} \kappa_a + \kappa_{as} & \kappa_a - \kappa_{as} & \gamma\eta_2(\kappa_a + \kappa_{\beta s}) & \gamma\eta_2(\kappa_a - \kappa_{\beta s}) \\ \gamma^*\eta_1(\kappa_b - \kappa_{as}) & \gamma^*\eta_1(\kappa_b + \kappa_{as}) & \kappa_b - \kappa_{\beta s} & \kappa_b + \kappa_{\beta s} \\ (\kappa_a - \kappa_{as})e^{-i\phi_{as}} & (\kappa_a + \kappa_{as})e^{i\phi_{as}} & \gamma\eta_2(\kappa_a - \kappa_{\beta s})e^{-i\phi_{\beta s}} & \gamma\eta_2(\kappa_a + \kappa_{\beta s})e^{i\phi_{\beta s}} \\ \gamma^*\eta_1(\kappa_b + \kappa_{as})e^{-i\phi_{as}} & \gamma^*\eta_1(\kappa_b - \kappa_{as})e^{i\phi_{as}} & (\kappa_b + \kappa_{\beta s})e^{-i\phi_{\beta s}} & (\kappa_b - \kappa_{\beta s})e^{i\phi_{\beta s}} \end{bmatrix}, \quad (B1)$$

$$G_s = \begin{bmatrix} 1 & 1 & \gamma\eta_2 & \gamma\eta_2 \\ \gamma^*\eta_1 & \gamma^*\eta_1 & 1 & 1 \\ e^{-i\phi_{as}} & e^{i\phi_{as}} & \gamma\eta_2 e^{-i\phi_{\beta s}} & \gamma\eta_2 e^{i\phi_{\beta s}} \\ \gamma^*\eta_1 e^{-i\phi_{as}} & \gamma^*\eta_1 e^{i\phi_{as}} & e^{-i\phi_{\beta s}} & e^{i\phi_{\beta s}} \end{bmatrix}, \quad (B2)$$

with all the parameters defined in the text. For p waves the situation is more involved due to the more complicated expressions for the polarization vectors. We obtain for the matrices

$$F_p = \begin{bmatrix} q_1\kappa_a + \bar{q}_1\kappa_{ap} & q_1\kappa_a - \bar{q}_1\kappa_{ap} & \gamma(q_3\kappa_a + \bar{q}_3\kappa_{\beta p}) & \gamma(q_3\kappa_a - \bar{q}_3\kappa_{\beta p}) \\ \gamma^*(q_2\kappa_b - \bar{q}_2\kappa_{ap}) & \gamma^*(q_2\kappa_b + \bar{q}_2\kappa_{ap}) & q_4\kappa_b - \bar{q}_4\kappa_{\beta p} & q_4\kappa_b + \bar{q}_4\kappa_{\beta p} \\ (q_1\kappa_a - \bar{q}_1\kappa_{ap})e^{-i\phi_{ap}} & (q_1\kappa_a + \bar{q}_1\kappa_{ap})e^{i\phi_{ap}} & \gamma(q_3\kappa_a - \bar{q}_3\kappa_{\beta p})e^{-i\phi_{\beta p}} & \gamma(q_3\kappa_a + \bar{q}_3\kappa_{\beta p})e^{i\phi_{\beta p}} \\ \gamma^*(q_2\kappa_b + \bar{q}_2\kappa_{ap})e^{-i\phi_{ap}} & \gamma^*(q_2\kappa_b - \bar{q}_2\kappa_{ap})e^{i\phi_{ap}} & (q_4\kappa_b + \bar{q}_4\kappa_{\beta p})e^{-i\phi_{\beta p}} & (q_4\kappa_b - \bar{q}_4\kappa_{\beta p})e^{i\phi_{\beta p}} \end{bmatrix}, \quad (\text{B3})$$

$$G_p = \begin{bmatrix} q_1 & q_1 & \gamma q_3 & \gamma q_3 \\ \gamma^* q_2 & \gamma^* q_2 & q_4 & q_4 \\ q_1 e^{-i\phi_{ap}} & q_1 e^{i\phi_{ap}} & \gamma q_3 e^{-i\phi_{\beta p}} & \gamma q_3 e^{i\phi_{\beta p}} \\ \gamma^* q_2 e^{-i\phi_{ap}} & \gamma^* q_2 e^{i\phi_{ap}} & q_4 e^{-i\phi_{\beta p}} & q_4 e^{i\phi_{\beta p}} \end{bmatrix}, \quad (\text{B4})$$

which contain the parameters

$$q_1 = -\frac{\alpha_{11}}{\kappa_{\parallel}} \{ \varepsilon + 6\gamma_0 + 3\gamma_0^2 \xi_1 \}, \quad (\text{B5})$$

$$q_2 = -\rho \frac{\alpha_{11}}{\kappa_{\parallel}} \{ \xi_1 (\varepsilon + 6\gamma_0) + 3 \}, \quad (\text{B6})$$

$$q_3 = -\frac{\beta_{21}}{\kappa_{\parallel}} \{ \xi_2 (\varepsilon + 6\gamma_0) + 3 \}, \quad (\text{B7})$$

$$q_4 = -\rho \frac{\beta_{21}}{\kappa_{\parallel}} \{ \varepsilon + 6\gamma_0 + 3\gamma_0^2 \xi_2 \}, \quad (\text{B8})$$

$$\bar{q}_1 = \frac{\alpha_{11}}{\kappa_{\parallel} \kappa_{ap}^2} \{ \kappa_{\parallel}^2 - (\varepsilon + 6\gamma_0) - 3\gamma_0^2 \xi_1 \}, \quad (\text{B9})$$

$$\bar{q}_2 = \rho \frac{\alpha_{11}}{\kappa_{\parallel} \kappa_{ap}^2} \{ \xi_1 [\kappa_{\parallel}^2 - \rho^2 (\varepsilon + 6\gamma_0)] - 3\rho^2 \}, \quad (\text{B10})$$

$$\bar{q}_3 = \frac{\beta_{21}}{\kappa_{\parallel} \kappa_{\beta p}^2} \{ \xi_2 [\kappa_{\parallel}^2 - (\varepsilon + 6\gamma_0)] - 3 \}, \quad (\text{B11})$$

$$\bar{q}_4 = \rho \frac{\beta_{21}}{\kappa_{\parallel} \kappa_{\beta p}^2} \{ \kappa_{\parallel}^2 - \rho^2 (\varepsilon + 6\gamma_0) - 3\gamma_0^2 \rho^2 \xi_2 \}. \quad (\text{B12})$$

-
- [1] B. Ya. Zel'dovich, V. I. Popovichev, V. V. Ragul'skii, and F. S. Faizullov, *JETP Lett.* **15**, 109 (1972).
[2] A. Yariv, *IEEE J. Quantum Electron.* **QE-14**, 650 (1978).
[3] D. M. Pepper, *Opt. Eng.* **21**, 156 (1982).
[4] *Optical Phase Conjugation*, edited by R. A. Fisher (Academic, New York, 1983).
[5] B. Ya. Zel'dovich, N. F. Pilipetskii, and V. V. Shkunov, *Principles of Phase Conjugation* (Springer, Berlin, 1985).
[6] M. C. Gower, *J. Mod. Opt.* **35**, 449 (1988).
[7] O. Yu. Nosach, V. I. Popovichev, V. V. Ragul'skii, and F. S. Faizullov, *JETP Lett.* **16**, 435 (1972).
[8] B. Ya. Zel'dovich, N. A. Mel'nikov, N. F. Pilipetskii, and V. V. Ragul'skii, *JETP Lett.* **25**, 36 (1977).
[9] R. W. Hellwarth, *J. Opt. Soc. Am.* **67**, 1 (1977).
[10] A. Yariv and D. M. Pepper, *Opt. Lett.* **1**, 16 (1977).
[11] D. M. Bloom and G. C. Bjorklund, *Appl. Phys. Lett.* **31**, 592 (1977).
[12] S. M. Jensen and R. W. Hellwarth, *Appl. Phys. Lett.* **32**, 166 (1978).
[13] P. V. Avizonis, F. A. Hopf, W. D. Bomberger, S. F. Jacobs, A. Tomita, and K. H. Womack, *Appl. Phys. Lett.* **31**, 435 (1977).
[14] J. Feinberg, *Opt. Lett.* **8**, 480 (1983).
[15] M. Cronin-Golomb, B. Fisher, J. O. White, and A. Yariv, *IEEE J. Quantum Electron.* **QE-20**, 12 (1984).
[16] G. Salamo, M. J. Miller, W. W. Clark III, G. L. Wood, and E. J. Sharp, *Opt. Commun.* **59**, 417 (1986).
[17] H. Kong, C. Lin, A. M. Biernacki, and M. Cronin-Golomb, *Opt. Lett.* **13**, 324 (1988).
[18] K. Sayano, G. A. Rakuljic, and A. Yariv, *Opt. Lett.* **13**, 143 (1988).
[19] P. M. Peterson and P. M. Johansen, *Opt. Lett.* **13**, 45 (1988).
[20] W. Krolikowski and M. R. Belic, *Opt. Lett.* **13**, 149 (1988).
[21] M. D. Ewbank, *Opt. Lett.* **13**, 47 (1988).
[22] A. Bledowski and W. Krolikowski, *Opt. Lett.* **13**, 146

- (1988).
- [23] M. R. Belic, *Phys. Rev. A* **37**, 1809 (1988).
- [24] J. Goltz, C. Denz, and T. Tschudi, *Opt. Commun.* **68**, 453 (1988).
- [25] Pochi-Yeh, *Introduction to Photorefractive Nonlinear Optics* (Wiley, New York, 1993).
- [26] H. F. Arnoldus and T. F. George, *Phys. Rev. A* **43**, 3675 (1991).
- [27] H. F. Arnoldus and T. F. George, *Phys. Rev. A* **43**, 6156 (1991).
- [28] J. D. Jackson, *Classical Electrodynamics* (Wiley, New York, 1962), p. 217.
- [29] Y. R. Shen, *The Principles of Nonlinear Optics* (Wiley, New York, 1984), Chap. 1.
- [30] M. Schubert and B. Wilhelmi, *Nonlinear Optics and Quantum Electronics* (Wiley, New York, 1984), p. 36.
- [31] D. A. Kleinman, *Phys. Rev.* **126**, 1977 (1962).
- [32] D. M. Pepper, D. Fekete, and A. Yariv, *Appl. Phys. Lett.* **33**, 41 (1978).
- [33] A. Yariv, *Optical Electronics*, 3rd ed. (Holt, New York, 1985), p. 506.
- [34] D. M. Pepper and R. L. Abrams, *Opt. Lett.* **3**, 212 (1978).
- [35] K. R. MacDonald and J. Feinberg, *Phys. Rev. Lett.* **55**, 821 (1985).
- [36] E. Wolf, L. Mandel, R. W. Boyd, T. M. Habashy, and M. Nieto-Vesperinas, *J. Opt. Soc. Am. B* **4**, 1260 (1987).
- [37] M. Segev, A. Yariv, and J. Shamir, *Opt. Lett.* **17**, 1076 (1992).
- [38] S. W. James, K. E. Youden, P. M. Jeffrey, R. W. Eason, P. J. Chandler, L. Zhang, and P. D. Townsend, *Opt. Lett.* **18**, 1138 (1993).
- [39] R. W. Boyd, *Nonlinear Optics* (Academic, Boston, 1992), p. 252.
- [40] B. Crosignani and A. Yariv, *J. Opt. Soc. Am. A* **1**, 1034 (1984).
- [41] A. A. Jacobs, W. R. Tompkin, R. W. Boyd, and E. Wolf, *J. Opt. Soc. Am. B* **4**, 1266 (1987).